RSC Advances

RSC Advances

www.rsc.org/advances

ROYAL SOCIETY OF CHEMISTRY

www.rsc.org/advances

RSC Advances

ARTICLE

Folate decorated delivery of self assembled betulinic acid nano fibers: A biocompatible anti-leukemic therapy

Sandeep Kumar Dash[a#], Shib Shankar Dash[b#], Sourav Chattopadhyay[a], Totan Ghosh[c], Satyajit Tripathy[a], Santanu Kar Mahapatra[d], Braja Gopal Bag[b], Debasis Das[c], Somenath Roy[a] *

[a]Immunology and Microbiology Laboratory, Department of Human Physiology with Community Health, Vidyasagar University, Midnapore-721 102, West Bengal, India.
[b] Department of Chemistry and Chemical Technology, Vidyasagar University, Midnapore, 721 102, West Bengal, India
[c]Department of Chemistry, University of Calcutta, 92, A. P. C. Road, Kolkata - 700 009, India
[d]School of Chemical & Biotechnology, SASTRA University, Thanjavur ‑ 613 401, Tamil Nadu, India.
# The authors are equally contributed to this work.

The objective of this study was to develop folate receptor mediated delivery of self assembled betulinic acid nano fibers (SA-BA) to human leukemic cells and to investigate their specific induction of apoptosis. The physicochemical properties of PEG conjugated SA-BA followed by conjugated with folic acid (FA-PEG-SA-BA) were examined using Fourier transform infrared spectroscopy, Thermogravimetry analysis, X-ray diffraction analysis, Thin layer chromatography and Scanning electron microscopy. The stability of folic acid with PEG-SA-BA conjugate was higher at acidic pH, which helps to maintain the conjugate structure for internalization of folate receptor over expressing cells. FA-PEG-SA-BA showed good compatibility with normal cells. The internalization of FA-PEG-SA-BA was significantly observed in folate receptor over expressing K562 cells while showing comparatively lower impact on folate receptor lower expressing KG-1A cells. This intracellular localization of conjugate facilitated the generation of excess reactive oxygen species (ROS), followed by elevation of tumor necrosis factor alpha (TNF-α) secretion. The effective contribution of ROS and TNF-α in FA-PEG-SA-BA mediated leukemic cell death was confirmed by pretreatment of cells with the ROS scavenger (N-acetyl-L-cysteine) and pentoxifylline, a potent TNF-α blocker. The mode of leukemic cell death was confirmed by flow-cytometric analysis. We also tested the possible involvement of caspase activation in TNF- α mediated leukemic cell death by immunoflouroscence staining of apoptotic marker proteins (caspase 8 and caspase 3).

1. Introduction

Natural product and naturally occurring substances plays a great role in anticancer drug development research [1-2]. Lower toxic effects and high selectivity are the two most important benefits of natural product based research.   Betulinic acid (BA), a naturally occurring pentacyclic lupine type triterpenoid is distributed among a wide range of plant Kingdome including *Tryphyllum peltatum, Ancistrocladus heyneaus, Diospyros leucomelas, Ziziphus jujube. (Rhamnaceae), Syzygium spp. (My- rtaceae)* etc [1,3]. Many bio-active secondary metabolites of plants, including BA induce apoptosis pathway in cancer cells to exert their selective cytotoxic effects. Previous studies showed that BA not only shows potent anti cancer effects, but also manifests anti-inflammatory, anti-HIV, anti-helmintic, anti-nociceptive activities [3-5]. The anticancer activity of

BA was observed significantly among various cancer cell types including carcinoma, melanoma, leukemic etc. [2,4]. Zuco et al [1] observed that BA specifically kills the tumor cells without producing any toxic impact on normal peripheral blood lymphocytes (PBL). Several studies were done over the last few years to illuminate the molecular mechanisms of BA mediated anti-cancer activity. The mechanism of BA mediated cytotoxicity is largely depends on its ability to trigger the mitochondrial pathway of apoptosis in cancer cells [2]. It was established that BA shows direct effect on mitochondria. Successive treatment of BA on cancer cells disrupts the mitochondrial transmembrane potential which facilitates the cells to undergo apoptosis. Involvement of excessive amount of ROS was found to be the most important factor for loss of mitochondrial membrane integrity of melanoma cells treated with BA [6]. BA directly targets to mitochondria, which in turn regulates the downstream caspase activation and side by side overcomes resistance property. [7] Thus, like other chemotherapeutic drugs, (doxorubicin, cisplatin etc.) BA has not developed resistance in cancer cells [8] and thereby became permissible agents for future cancer therapy. Ehrhardt et al (2004) showed that BA produced noticeable apoptosis in 65% of primary pediatric acute leukemia cells with different leukemic cell lines used in this study. The same study also showed that BA was more potent than nine out of 10 standard anti-cancer drugs and exerted greatest efficiency in tumor relapse. Preferential killing and targeted delivery via selective cellular markers can highly increase the potency as well as reduce the toxicity of therapeutic agents [9]. Among receptor mediated targeted delivery system, the folate receptor (FR) mediated delivery system gain maximum attention of many researchers [11-13]. Folate receptor (FR) is a glycosylphosphatidylinositol (GPI) anchored cell surface glycoprotein. There are four isoforms of this receptor family have been identified and are classified as folate receptor alpha (FRα), beta (FRβ), delta (FRΔ) and gamma (FRγ), respectively. Folate receptor alpha (FRα), beta (FRβ) isoforms are both GPI-anchored proteins contain two N-glycosylation sites and comprise high affinity for folic acid/vitamin B9 [14-15]. It was found that expression of FR-α is frequently augmented in various types of epithelial cancers, whereas FR-β expression is noted in myeloid leukemia and chronic inflammatory diseases [9]. Physical conjugation of chemotherapeutic with folic acid preferentially internalized by folate receptor over expressing cancer cells and thereby killed them without showing any toxic effects on normal cells [16].

Though some of the study was performed earlier to evaluate the cytotoxic potential of BA on human myeloid leukemia [17-18], but till to date not a single study have been undertaken regarding the folate receptor mediated targeted delivery of BA in human myeloid leukemia cells. In this study, we have successfully functionalized the self assembled betulinic acid (SA-BA) with PEG (polyethylene glycol) followed by conjugation with folic acid (Supporting information Scheme S1). It was well established that PEG fictionalization protects the particles from uptake of the reticulo-endothelial system (RES) and thereby increases long circulating time. Conjugation of folic acid with PEG functionalized SA-BA were performed to facilitate the folate receptor mediated targeted delivery of SA-BA on KG-1A (Human acute myeloid leukemia cells) and K562 (Human chronic myeloid leukemia cells).

2. Result and Discussion

2.1 Encapsulation efficiency (EE) and loading capacity (LC)

The EE and LC of PEG with SA-BA were found to be 86.47% and 74.31% respectively. It was observed that EE and LC of FA with PEG-SA-BA is depends on FA concentration. When 1.5 mg of FA was conjugated with PEG-SA-BA then the EE became 61.77% which was elevated to 96.22% when 2.5 mg FA was used. The LC was also significantly (p<0.05) elevated like this manner. When 2.5 mg FA were used the LC became 83.66% (Supporting information Table S1). The initial concentration of FA plays an important role in the encapsulation efficiency and loading capacity of PEG-SA-BA. When the concentration of FA was increased, the EE and LC with PEG-SA-BA conjugate were increased. Higher EE and LC are the two basic needs for drug targeting and delivery. Based on the result the highest EE and LC contained conjugate was selected for further assays.

2.2 Estimation of FA stability with the conjugate

Stability of FA with PEG-SA-BA was investigated using duration dependant FA release percentage on pH 5.4, 7.4 and 9.0. It was manifest that at acidic pH (pH 5.4) the conjugate was highly stable. Very lower amount of FA (<30%) was released at 48 hr. The FA release was slightly elevated at pH 7.4 and maximal was observed at pH 9.0 (>70%) at 48 hr incubation (Fig. 1). The FA release assay suggested that the FA-PEG-SA-BA conjugate was highly stable at acidic pH which is present in the cancer cell microenvironment [19]. Previous studies showed that BA didn't take up by normal cells [1] and healthy cells and they are expressing little or no folate receptors [19]. Thus, at physiological pH (normal cell growth environment) slight increased of FA release was noted which might give rise to completely non-toxic effects of the conjugates towards PBL. At highly alkaline pH the FA were significantly released from the conjugate which clearly demonstrated the instability of the conjugate at alkaline environment.
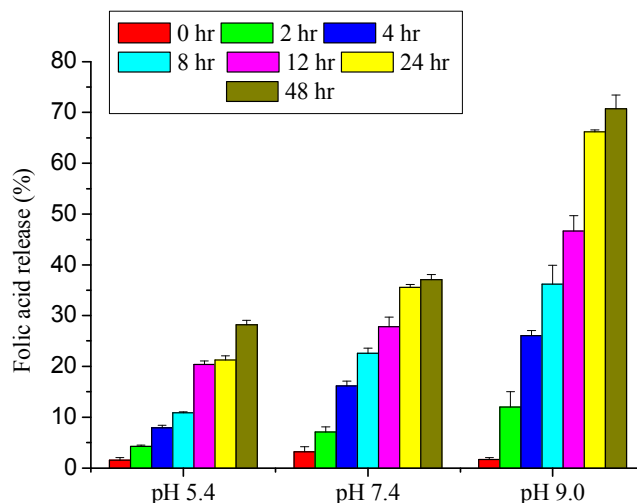
Figure 1: pH based stability assay of FA-PEG-SA-BA. FA-PEG-SA-BA was dissolved in different pH solution and subsequently incubated for 48 hr. Release of folic acid in supernatant medium was evaluated spectrophotometically at 546 nm.

2.3 Physical Characterization

2.3.1. FTIR and DFT studies to prove the conjugate structures: DFT of optimized structures of SA-BA and PEG (for simplicity we have taken n = 1) and mixture of SA-BA, FA and PEG were performed to establish their supramolecular arrangement as well as IR behavior. The optimized structure of

the mixture of SA-BA and PEG depicted in Fig. 2A indicated that in the lower energy conformation SA-BA and PEG are connected through H-bonding [hydrogen of hydroxyl group (-OH) of SA-BA involve in H-bonding with oxygen of PEG] [57]. This also supported by experimental IR of SA-BA and experimental and theoretical IR spectrum of the mixture of SA-BA and PEG (Supporting information Fig. S1). In the same scenario, all the component in the mixture of SA-BA, FA and PEG are inter-connected through H-bonding (Fig. 2B). In the optimized structure of the mixture of SA-BA, FA and PEG, carbonyl oxygen (-C=O) of carboxylic acid group (-COOH) of FA are involve in H-bonding with the hydroxyl group of PEG. So the ν(C=O) of FA appear slightly lower region [1685 cm-1 (exp.); 1680 cm-1 (theo.)] in mixture 2 than that in free folic acid [1698 cm-1 (exp.)] (Fig. 3).
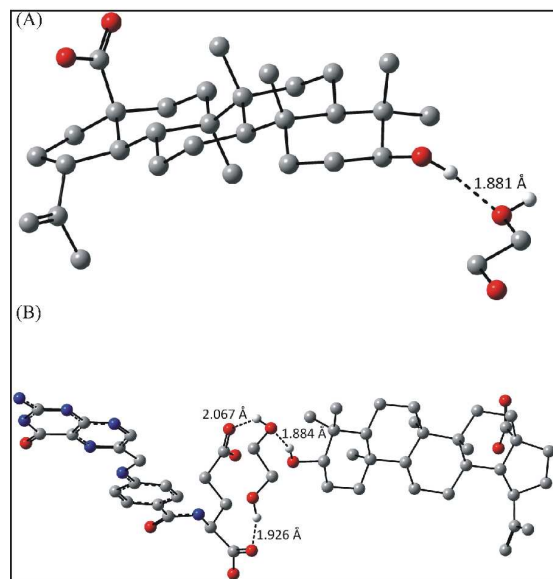

Figure 2: Optimized structures of (**A**) mixture of SA-BA and PEG (PEG-SA-BA) and (**B**) mixture of SA-BA, FA and PEG (FA-PEG SA-BA).
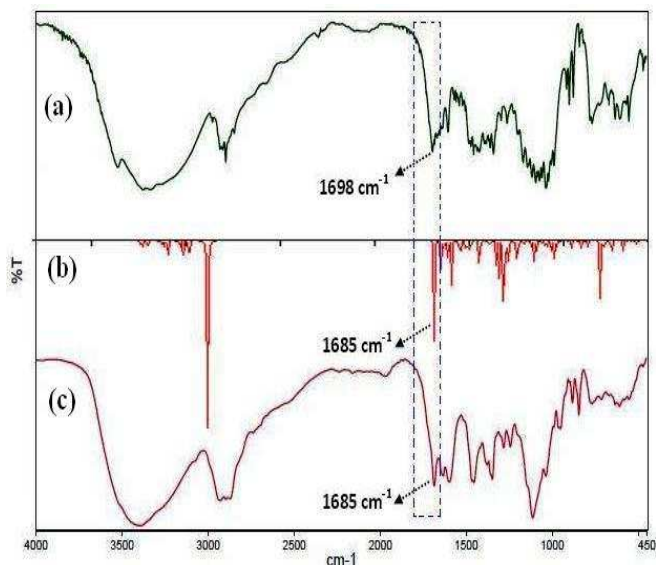

Figure 3: FTIR spectrum: (a) Folic acid, (b) theoretical FTIR of the mixtue of SA-BA, ethylene glycol and folic acid, and (c) experimental FTIR of SA-BA, ethylene glycol and folic acid.

2.3.2. Thin layer chromatography (TLC) identification: TLC is one of the useful procedures for identity, quality evaluation as well as quantitative determination of molecules. PEG and FA are highly polar, so we used 50% ethanol/ethyl acetate solvent system to move the spot away from base of TLC plate. In PMA stain the blue spots were appeared for SA-BA and FA-PEG-SA-BA (Supporting information Fig. S2A), because the large number of $-CH_2$ groups present in the acid get oxidized by PMA. PEG and FA remain inert in PMA stain, but spots appeared when exposed to iodine vapor (Supporting information Fig. S2B).

2.3.3.Thermogravimetry analysis: Critical thermogravemetric analyses suggested that the compound (FA-PEG-SA-BA) has no thermally end product at/ after 550° C as the compound is an organic one. At very low temperature FA decomposes, then SA-BA and finally PEG which may conclude from their structural geometry (Supporting information Fig. S3A and Fig.S3B). Solid state thermal analyses were performed in order to (i) understand the thermal decomposition patterns of the compound, (ii) to verify the molecular composition of the compound and (iii) to synthesize the thermally stable end products. From DTA curve, we obtained that each step of weight loss by the compound was exothermic in nature.

2.3.4. X-ray diffraction analysis: X-ray diffraction pattern of the FA-PEG-SA-BA conjugate exhibited sharp peaks, which usually characterize crystalline compounds [20]. The diffractogram of the physical mixture of BA and FA and PEG (Supporting information Fig. S4) practically represents the sum of the individual diffractograms, [21-22] revealing the peaks at a lower intensity compared with the pure compound in direct proportionally with its concentration in the mixture. The presence of the peaks at 18.6°, 19.4°, and 22.7° suggested that the structure of the folic acid and BA did not change too much internally. Interestingly, the position of the new peaks differs very little compared to the pure substance or its physical mixture. The disappearance of some peaks and appearance of new peaks of different intensity and position can be considered evidence of real inclusion complex formation. Given the inclusion of BA and FA inside of the cavity of PEG as a result, some BA and FA-related peaks have disappeared, and a new compound emerged, characterized by a completely new X-ray profile (Supporting information Fig. S4).

2.3.5. Scanning electron microscopy: The morphology of the SA-BA and FA-PEG-SA-BA was investigated using SEM imaging. SEM imaging revealed that in ethanol-water mixtures FA-PEG-SA-BA produced several fibrillar networks. The single fiber of FA-PEG-SA-BA had the nanometer cross sections (10-20 nm) and micrometer lengths (1-3 micrometer). In this cases the fibers were aggregated together to form 3D network structure (Fig. 4). In ethanol-water (16:4, 0.5% w/v) mixture BA becomes self assembled which we have previously reported [23]. In the present study, SEM images revealed that even after conjugation with PEG and FA, the self assembled property of BA was maintained.
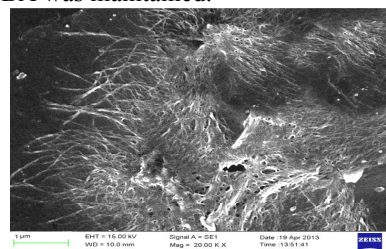
Figure 4: SEM images of FA-PEG-SA-BA in ethanol-water mixture (16:4)

2.3.6. ^{1}H NMR of PEG-SA-BA and FA-PEG-SA-BA conjugates: In the ^{1}H-NMR spectrum of PEG conjugated SA-BA we observed that the presence of characteristic peaks for both the betulinic acid and PEG, which indicated that the formation of PEG-SA-BA conjugate (Supporting information Fig. S5). Similarly, on comparison of ^{1}H NMR spectrum of FA-PEG-SA-BA conjugate with the ^{1}H NMR spectrum of SA-BA, PEG and FA, we observed the presence of characteristic peaks for SA-BA, PEG and FA (Supporting information Fig. S8, S9 and S10 respectively) in the ^{1}H NMR of final compound which was an indicative for the formation of stable FA-PEG-SA-BA conjugate (Supporting information Fig. S11).

2.3.7. Dynamic light scattering and surface zeta potential measurement: The size distribution of FA-PEG-SA-BA suspended in aqueous medium was characterized by DLS. The hydrodynamic size (Z-average) of the conjugate was 92.39 nm with a polydispersity index (PDI) of 0.439 (Supplementary information Fig. S6). The zeta-potential measurement showed that FA-PEG-SA-BA had a negative zeta potential (-25.6 mV), indicating that the conjugate possess a negatively charged surface (Supplementary information Fig. S7).

2.4 Cell viability study

Cell viability study of DOX, PEG-SA-BA, FA-PEG-SA-BA on PBL, KG-1A (FR –ve) and K562 (FR +ve) cells carried out to estimate the cell killing ability of the applied drugs. In our study, treatment with DOX significantly ($p < 0.05$) decreased the viability of PBL from 5µg/ml to last dose. In the same line of treatment, it killed the leukemic cells significantly ($p < 0.05$) by all doses used (Fig. 5A). PEG-SA-BA and FA-PEG-SA-BA did not produce any significant cell death of PBL at any doses used. PEG-SA-BA was able to kill the KG-1A cells significantly ($p < 0.05$) by 42.01%, 58.16%, 77.33%, 80.51% were as FA-PEG-SA-BA killed these cells significantly ($p < 0.05$) by 56.01%, 61.16%, 83.33% and 84.51% at 10, 15, 20 and 25 µg/ml doses respectively (Fig. 5B and Fig. 5C). In case of K562 cells, PEG-SA-BA was able to significantly ($p < 0.05$) kill the K562 cells by 38.42%, 44.36%, 62.90%, and 64.45% were as FA-PEG-SA-BA killed these cells significantly ($p < 0.05$) by 58.62%, 74.41%, 89.35%, and 88.76% at 10, 15, 20 and 25 µg/ml doses respectively (Fig. 5B and Fig. 5C). The IC_{50} value of DOX, PEG-SA-BA and FA-PEG-SA-BA against PBL, KG-1A and K562 cells were found to be 9.61, 3.32 and 2.89µg/ml, respectively, for the DOX and 242.58, 12.92, 16.41µg/ml, respectively for PEG-SA-BA, and 153.47, 11.52, 10.31 µg/ml respectively for FA-PEG-SA-BA after interaction for 24 hours. So, from this study the 15 µg/ml dose of PEG-SA-BA and FA-PEG-SA-BA was selected as biological safe dose for further assay. The present cell viability study showed that FA-PEG-SA-BA did not produce a significant elevation of cell killing activity in comparing to PEG-SA-BA on KG-1A cells, but in case of K562 cells the opposite effects were noted. Here, Folic acid receptor presence may play a vital role in the derivative action of those two drugs. The presence of higher level of FR in K562 cell surfaces may facilitate the higher internalization of FA-PEG-SA-BA in K562 cells [24], so cell viability was drastically reduced in this cell type. On the other hand KG-1A cells are FR negative cells, so both the drugs, PEG-SA-BA and

FA-PEG-SA-BA showed nearly similar cytotoxic effects on these cells. Based on the results obtained from cell viability assay, FA-PEG-SA-BA was only selected for further experiments.

2.5 Drug internalization

Internalization of FA-PEG-SA-BA was examined by fluorescence microscopy images. Successful tagging of Rh-B with FA-PEG-SA-BA was confirmed by fluorescence images (Fig. 6). The fluorescence imaging showed that higher amounts of FA-PEG-SA-BA were internalized in K562 cells. No significant amounts Rh-B fluorescence intensity in PBL was noted. This differential uptake of FA-PEG-SA-BA in KG-1A and K562 cells give strong evidence for folate receptor mediated delivery of PEG protected SA-BA. Higher internalization of FA-PEG-SA-BA in FR positive K562 cells supports the higher cell death in comparing to lower FR expressing KG-1A cells. Normal cells are expressing little or no folate receptors [19]. Thus very lower Rh-B intensity in PBL for both the drugs supports the non-toxic property of BA on normal cells, which is previously reported by many researchers [1,25-26]. This selective internalization of both drugs in leukemic cells may be due to receptor mediated endocytosis. [24,27] Both drugs were distributed in leukemic cells throughout the cells indicated that cellular uptake were confirm processed instead of adhering to the cell surfaces.

2.6 Compatibility with human RBCs

To investigate any hemolytic activity of FA-PEG-SA-BA, human normal RBCs were treated with FA-PEG-SA-BA at varying doses (0-100µg/ml) for 3 hours. It was observed that FA-PEG-SA-BA did not produce any hemolytic activity upto 50 µg/ml dose. At 100µg/ml dose this drug showed significant ($p < 0.05$) elevation of hemolytic activity (53.52%) when compared with the negative control (Fig. 7). The non-hemolytic activity of FA-PEG-SA-BA suggested that this drug was completely compatible with normal RBCs. So the selected dose (15µg/ml) in our study is the biological safe dose for SA-BA delivery. A very recent study of Gao et al. [28] reported that the IC_{50} value for BA induced hemolysis in human RBCs was 60 µM. Thus, in our study, having a much lower amount of drug used (15 µg/ml), where no hemolytic activity was noted upto 50 µg/ml dose.

2.7 Phagocytosis of the drug by macrophages in vitro

The phagocytosis of FA-PEG-SA-BA by macrophages was studied *in vitro*. It was observed that phagocytosis of the folate conjugated drug by macrophages was substantially lower, as compared to the uptake by leukemic cells (Fig.8 and Fig 5). Macrophages are the primary phagocytic cells present in the body, which play a crucial role in the clearance of particles delivered into the body's circulation. So the protection of the applied drugs from macrophages is one of the essential needs for drug delivery. It was reported that surface conjugation with PEG lowers the changes of phagocytosis and enriches the long circulating time [29]. At the same time conjugation of drugs with folic acid makes it selective for FR positive cells (K562 cells) only. FR is minimally distributed on macrophages and having

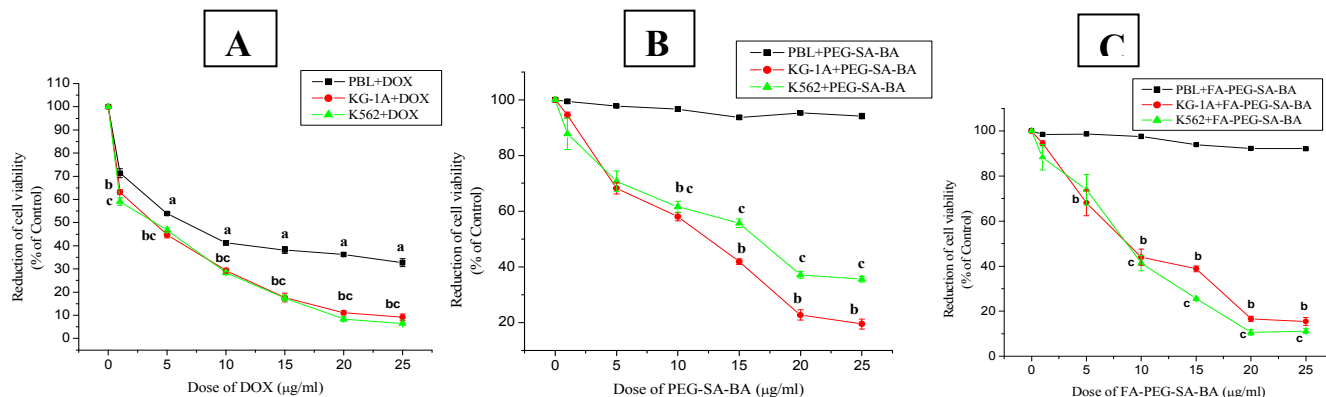the presence of PEG the FA-PEG-SA-BA was not significantly localized in macrophages. [30-31]

Figure 5: In vitro cell viability assay of DOX (**A**), PEG-SA-BA (**B**) and FA-PEG-SA-BA (**C**) treated PBL, KG-1A and K562 cell lines. Cells were treated with DOX, PEG-SA-BA and FA-PEG-SA-BA for 24 h at 37 °C. Cell viability was measured by the MTT method as described in materials and methods.

2.8 Lactic dehydrogenase release

Lactic dehydrogenase is a marker enzyme for cell viability as well as plasma membrane integrity. In our study, the significant LDH release was noted after 24 hr incubation period for KG-1A and K562 cells in the selected concentration of FA-PEG-SA-BA (15 μ g/ml) (Fig. 9). In KG-1A cells LDH release was significantly elevated by 42.74 % and by 59.65 % in K562 cells as compared with the control group. No significant LDH release was noted for PBL. On the other hand DOX showed higher elevation of LDH in all cells tested as compared to control and FA-PEG-SA-BA treated cells. The increase of LDH leakage in medium was due to rapid cell-membrane lysis which leads to cell death and suggested that the membrane leakage was a consequence of the apoptosis [32]. Evidence of BA mediated cell death through elevation of LDH release was reported earlier by previous study [33] and those findings highly support the present outcome. Treatment with FA-PEG-SA-BA did not significantly alter the LDH level in PBL, supports the nontoxic natures of the conjugate and corroborate with the report of Viji et al [34].
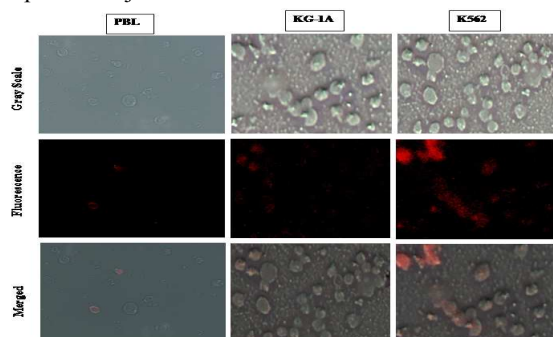

Figure 6: Intracellular uptake of FA-PEG-SA-BA on PBL, KG-1A and K562 cells by fluorescence imaging. A required amount of cells was treated with Rhodamin B labeled FA-PEG-SA-BA (15 µg ml⁻¹) for 6 h. Intracellular uptake was examined using fluorescence microscope.

2.9 Cellular oxidative stress

PBL, KG-1A and K562 cells were treated with FA-PEG-SA-BA (15 µg/ml), and ROS were deliberated by conversion of

H$_2$DCFDA for 2,7-dichloroflurescein (DCF). Results showed that FA-PEG-SA-BA treatment leads to significant (p<0.05) increase of ROS formation inside KG-1A and K562 cells by 4.90 fold and 6.48 fold respectively, compared with respective control cells (Fig.10 A and Fig. 10 B). Treatment with DOX was also exhibited high level (6.66 Fold in KG-1A and 7.28 fold in K562 cells) of intracellular ROS generation. The main difference was noted in PBL. In PBL, DOX treatment also significantly (p<0.05) elevated ROS level by 5.2 fold, but FA-PEG-SA-BA treatment has not significantly altered ROS level in PBL as compared to control cells. Most of the drugs induce apoptosis through the generation of ROS inside cells, which in turn leads to oxidative damages of the DNA molecule. Excess production of ROS and subsequent DNA damage, facilitate the process of topoisomerase I–DNA cleavable complex trapping in cells, which intern activates apoptotic processes through cleavage of caspases [36] When leukemic cells (KG-1A and K562) were pre-treated with NAC before the treatment with FA-PEG-SA-BA, the cell viability was significantly restored as compared with the result of cell viability assay where only FA-PEG-SA-BA was used and no such pre-treatment were done. In case of KG-1A cells, pre-treatment of NAC protected the cells from FA-PEG-SA-BA exposure and the cell viability was noted as 71.84%, 76.20% and 86.97%, 93.10% at 5 mM and 10mM NAC exposure respectively in KG-1A and K562 cells (Fig.11). PBL was not taken for this experiment as it did not show significant cell death in FA-PEG-SA-BA treatment. The effective contribution of ROS in FA-PEG-SA-BA mediated cytotoxicity in leukemic cells was examined by NAC pretreatment. Significant restoration of cell viability in NAC pretreatments suggested that the leukemic cell killing by FA-PEG-SA-BA was surely due to the generation of excess ROS production.
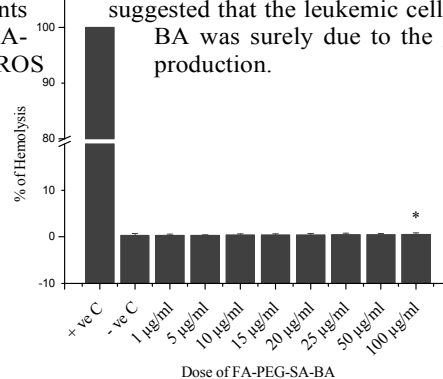
Figure 7: Estimation of haemolytic activity of FA-PEG-SA-BA. Human RBCs were treated with varying concentration of SA-BA (1-100 µg/ml). The absorbance of the supernatants at 570 nm was determined by using a microplate reader with the absorbance at 655 nm as a reference. The result was expressed as percentage of hemolysis as compared to control groups
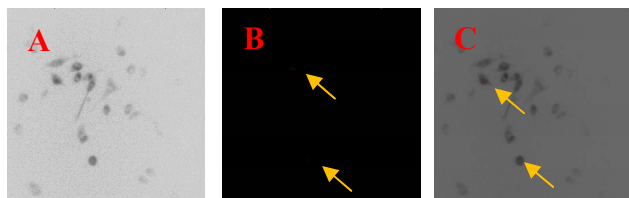

Figure 8: Estimation of phagocytic uptake of FA-PEG-SA-BA particles by RAW 264.7 cells. A required amount of cells was treated with Rhodamin B labeled FA-PEG-SA-BA (15 µg ml^{-1}) for 6 h. Intracellular uptake was examined using fluorescence microscope.

2.10 Detection of apoptosis and associated nuclear morphological changes

To determine whether the growth inhibitory activities of FA-PEG-SA-BA were related to the induction of apoptosis, the morphological changes of KG-1A and K562 cells were investigated using acridine orange/ethidium bromide (AO/EB) staining and apoptosis associated nuclear morphological abnormalities were observed by DAPI staining. Results showed that treatment with FA-PEG-SA-BA on KG-1A and K562 significantly increased the number of early and late apoptotic cells as evidenced by a bright green nucleus with condensed or fragmented chromatin and condensed orange-red chromatin respectively (Fig. 12A). In case of DAPI staining (as shown in Fig. 12B), leukemic cells treated with FA-PEG-SA-BA for 24 h exhibited significant increased in nuclear fragmentation and chromatin condensation phenomenon Apoptosis is a physiological blueprint of cell death characterized by morphological features and widespread DNA fragmentation [37]. Cancer cells are devoid of apoptosis. Thus, induction of apoptosis is the most important key factor for anticancer strategy. In our study induction of apoptosis in leukemic cells by FA-PEG-SA-BA was monitored by Et-Br/AO and DAPI staining. AO is taken up by both viable and non-viable cells and emits green fluorescence when intercalated into double stranded DNA. Et-bar is taken up only by non-viable cells and emits orange, red fluorescence by intercalation into DNA. On the other side nuclear condensation or fragmentation as evident by DAPI staining is another major evidence of apoptosis, leading to caspage activation. Collectively, these results demonstrate that FA-PEG-SA-BA inhibited cell growth and induced selective apoptosis in KG-1A and K562 cells.
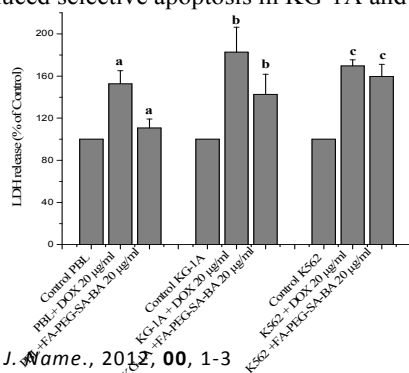

Figure 9: LDH release level of DOX treated and FA-PEG-SA-BAtreated PBL, KG-1A and K562 cell lines. The levels of LDH were expressed as percentage of untreated cells. Values are expressed as mean ± SEM of three experiments; superscripts indicate significant difference (p < 0.05) compared with the control group.

2.11 Assessment of apoptotic cell population by flowcytometry

Dual staining analysis of Annexine V+FITC fluorescence (FL1) and PI fluorescence (FL3) gave different cell populations wherein FITC negative and PI negative cells were selected as viable cells, FITC positive and PI negative were apoptotic and FITC positive and PI positive were defined as late apoptotic [38]. Only PI positivity showed necrotic or completely dead cell populations. As it was evident from Fig. 14, KG-1A and K-562 cells treated with 15µg/ml FA-PEG-SA-BA showed increased Annexin-V positivity. Maximum numbers of the cells gave both FITC and PI signals which suggested the cells undergoing late stage apoptosis. An increase was also noted in the PI positive population in the early stages of treatment, which clearly documents that FA-PEG-SA-BA induced the changes in cell membrane permeability. In case of PBL, FA-PEG-SA-BA treatment did not show any significant apoptotic or necrotic effects. (Fig. 13)
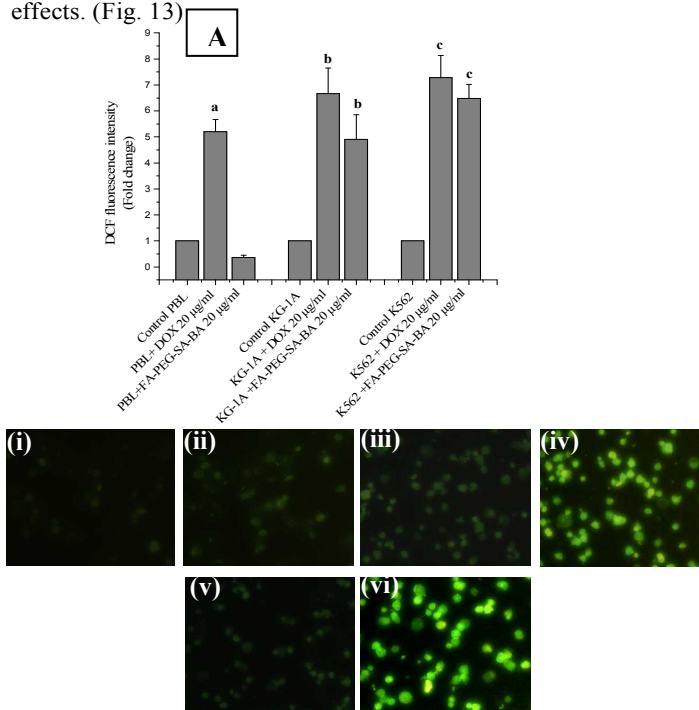
Figure 10: **A**: Effects of DOX and FA-PEG-SA-BA on ROS induction in PBL, KG-1A and K562 cell lines. DCF fluorescence intensity was expressed in term of ROS production. Results represent the means of three separate experiments, and error bars represent the standard error of the mean. Values are expressed as mean ± SEM of three experiments; superscripts indicate significant difference (p < 0.05) compared with the control group. Intensity of control cells were set to 100. Data is represented as the percentage of the ROS level in the control group.

B: (i-vi). Qualitative characterization of reactive oxygen species formation by DCFH$_2$-DA staining using fluorescence microscopy. After the said treatment schedule leukemic were incubated with DCFH$_2$-DA. At the end of DCFH$_2$-

DA exposure, cells were washed with PBS and they were visualized by fluorescence microscopy at an excitation wavelength of 485 nm and an emission wavelength of 520 nm. Here, **(i)**: PBL control, **(ii)**: FA-PEG-SA-BA treated PBL, **(iii)**: KG-1A control, **(iv)**: FA-PEG-SA-BA treated KG-1A cells, **(v)**: K562 control and **(vi)**: FA-PEG-SA-BA treated K562.

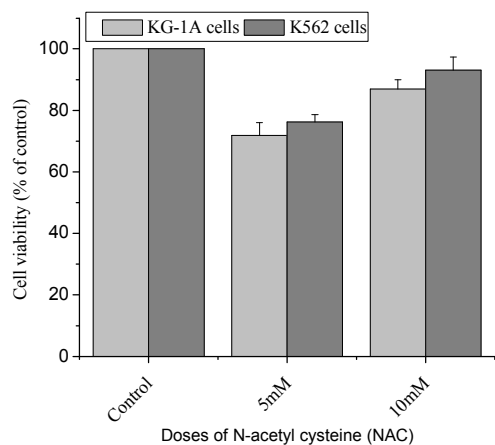**Figure 11:** Quenching of ROS rescues KG-1A and K562 cells from FA-PEG-SA-BA induced cytotoxicity. KG-1A and K562 cells were pre-treated with 2 and 5mM NAC for 4-6 hrs and then subsequently exposed to FA-PEG-SA-BA 15 µg/ml dose. Cell viability was estimated by MTT assay.

2.12 Involvement of TNF-α in FA-PEG-SA-BA induced cytotoxicity in leukemia cells

It was previously established that TNF-α is highly responsible for generate of ROS and activate the downstream apoptosis signals. In our study elevated level of TNF-α was noted due to exposure of FA-PEG-SA-BA in both cell types (Fig. 14A). Thus, to observe the role of TNF-α on FA-PEG-SA-BA induced cancer cell (KG-1A and K562) killing, we co-culture the both leukemia cells with 1 and 2mM POF (a potent TNF-α inhibitor) and FA-PEG-SA-BA (15 µg/ml) (Fig. 14B). The viability was estimated by MTT method. It was observed that POF played an immense role in eliminating toxic effects induced by FA-PEG-SA-BA in both leukemic cells. In each case cell viability was >92%. Previous studies showed that TNF-α initiates many downstream signaling pathways, including NF-κB activation, MAP kinase activation and the induction of both apoptosis and necrosis [39]. TNF-α is a pleiotropic cytokine, induces either cell proliferation or promote cell death. Release of TNF-α is highly correlated with NF-kappaβ activation. Inhibition of NF-kappaβ activation results in susceptibility to TNFα-induced death, associates with sustained JNK activation, an important donor to the death response [40]. TNF-α has shown to escort to ROS generation through the activation of NADPH oxidase by mitochondrial pathways, or other enzymes. ROS produced by TNF-α have an important function in cell death by activating c-Jun N-terminal kinase pathway [41]. Thus, in our study blocking of TNF-α completely blocked the TNF-α and ROS mediated cell death and thereby suggested the possible role of TNF-α and ROS in FA-PEG-SA-BA induced cytotoxicity towards both leukemic cells (KG-1A and K562).

2.13 Immuno flouroscence staining of apoptotic marker proteins

Significantly higher expression of caspage 8 and 3 proteins in FA-PEG-SA-BA treated leukemic cells was observed from their respective fluorescence images (Fig. 15) compared with untreated cells. Elevated expression of those pro-apototic marker proteins in FA-PEG-SA-BA treated KG-1A and K562 cells suggested the activation of apoptosis phenomenon. It was well established that higher expression of inflammatory cytokines mainly TNF-α is an established stimulator of the caspase 8 pathway [42]. Caspase-3 has been known as key executioners of apoptosis, being responsible either partially or totally for the proteolytic cleavage of many key proteins, including nuclear enzyme poly (ADP ribose) polymerase (PARP). Thus the results from the study also indicated that FA-PEG-SA-BA activated caspases 8 and thereby activated caspase 3 which ultimately leads to apoptotic cell death in KG-1A and K562 cells (Fig. 15).
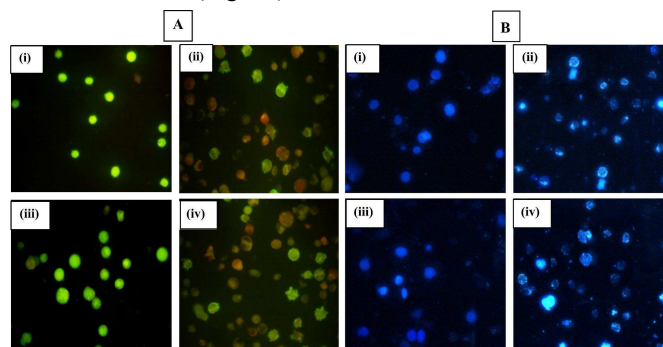
Figure 12: Qualitative characterization nuclear morphology by EtBr/AO (**A**) and DAPI (**B**) staining using fluorescence microscopy. After the treatment schedule PBL and leukemic cells were incubated with EtBr/AO and DAPI. At the end of EtBr/AO and DAPI exposure, cells were washed with PBS and they were visualized by fluorescence microscopy at excitation/emission wave length 490/620 nm and 345/455nm respectively. Here, **(i)**: KG-1A control, **(ii)**: FA-PEG-SA-BA treated KG-1A cells, **(iii)**: K562 control and **(iv)**: SA-BA treated K562 cells.
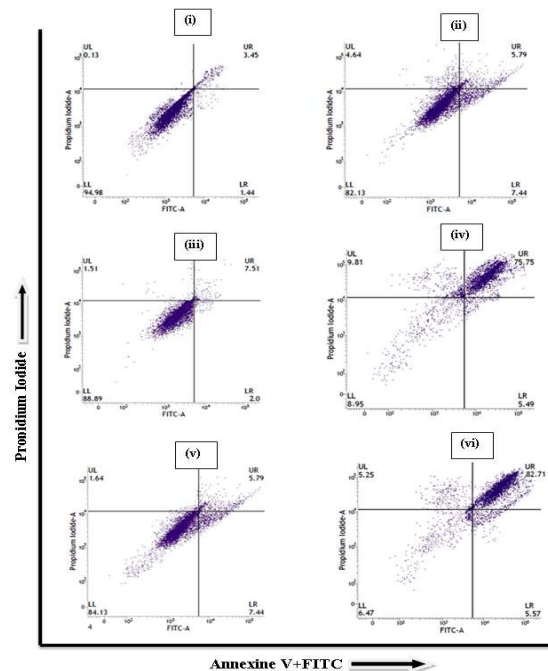
Figure 13: Estimation of apoptotic cell population by FACS using Annexine-V/PI staining. The percentage of cell population of PBL, KG-1A and K562 cells at Sub G0, G0/G1, S and G2/M was estimated before and after FA-

PEG-SA-BA treatment. Values are expressed as mean. Here, **(i)**: PBL control, **(ii)**: FA-PEG-SA-BA treated PBL, **(iii)**: KG-1A control, **(iv)**: FA-PEG-SA-BA treated KG-1A cells, **(v)**: K562 control and **(vi)**: FA-PEG-SA-BA treated K562.

Figure 14: Estimation of TNF-α level by ELISA (**A**). Inhibition of TNF-α production protects the KG-1A and K562 cells from FA-PEG-SA-BA -induced cytotoxicity (**B**). KG-1A and K562 cells were pre-treated with 1mM Pentoxifylline (POF), a 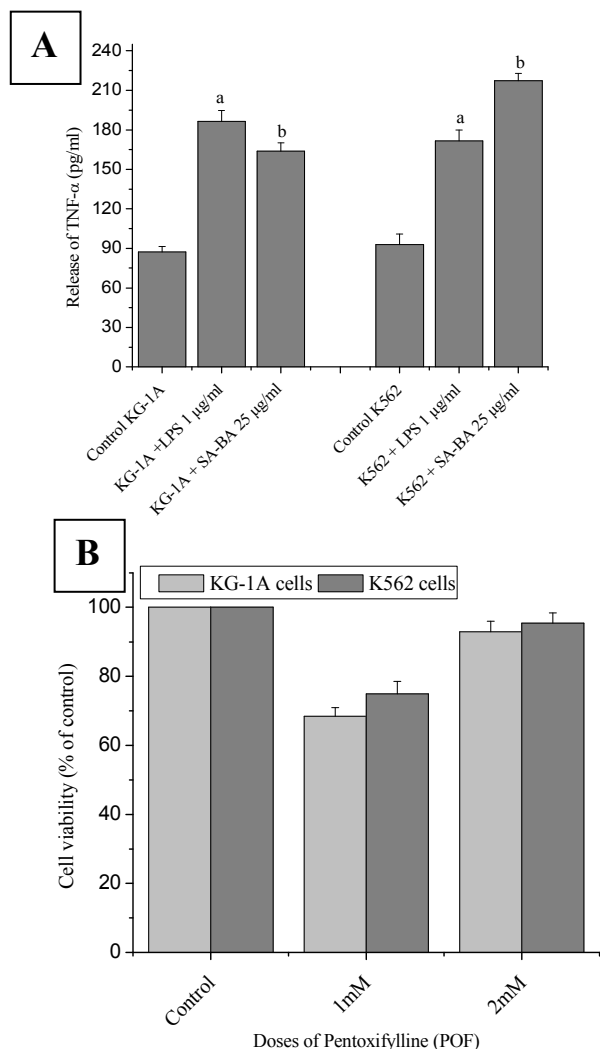potent TNF- α inhibitor for 24 hrs and then subsequently exposed to FA-PEG-SA-BA 15 µg/ml dose. Cell viability was estimated by MTT assay.
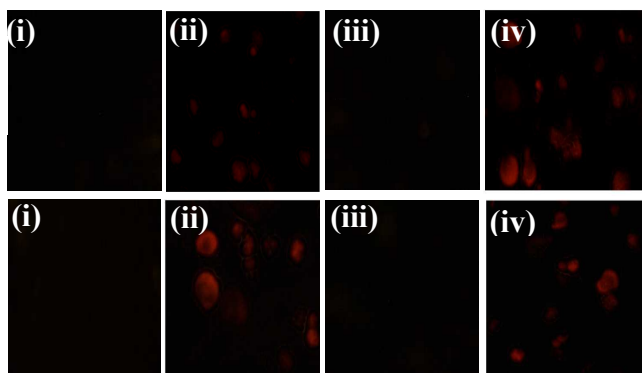

Figure 15: Detection of pro-apoptotic protein expression by immunoflourescence staining. KG-1A and K562 cells were treated with FA-PEG-SA-BA (15µg/ml) for 24 hr. After the treatment schedule cells were incubated with anti caspase 8 and 3 antibodies and subsequently exposed to rhodamine-conjugated compatible secondary antibodies for 1 h at 25^{0}C. Cells were visualized by fluorescence microscopy. Here: **(i)**: FA-PEG-SA-BAtreated KG-1A cells **(ii)**: FA-PEG-SA-BA treated K562 cells, **(iii)**: FA-PEG-SA-BA treated KG-1A cells **(iv)**: FA-PEG-SA-BA treated K562 cells.

3. Experimental Section

3.1 Culture media and chemicals

Histopaque 1077, and Rhodamine B, RPMI 1640, penicillin, streptomycin, pentoxifylline (POF), N-acetyl-L-cysteine (NAC), PEG$_{6000}$, doxorubicin were procured from Sigma (St. Louis, MO, USA). Fetal bovine serum (FBS) was purchased from GIBCO/Invitrogen. MTT was purchased from Himedia, India. Zinc perchlorate hexahydrate, Tris–HCl, Tris buffer, Titron X-100, Sodium dodecyl sulphate (SDS), phenol, chloroform, iso-amyl alcohol, ethidium bromide (EtBr), 2-vinylpyridine were procured from Merck Ltd., SRL Pvt. Ltd., Mumbai, India. Commercially available dimethyl sulfoxide (DMSO) was procured from Hi-media, India, and was purified by vacuum distillation over KOH. All other chemicals were from Merck Ltd and SRL Pvt. Ltd. Mumbai, were of the highest purity grade available.

3.2 Extraction and purification of Betulinic acid

Extraction, purification and isolation of BA was reported in our previous study [23].

3.3 Physical measurements

Purified BA was characterized earlier by the ^{1}H NMR, ^{13}C NMR, FTIR, XRD and Reversed-phase HPLC analysis. Self assembled property of BA was examined by Optical polarized microscopic images (OPM), Scanning electron microscopy (SEM), Atomic force microscopy Images (AFM), X-Ray Diffraction (XRD) studies were previously reported [23].

3.4. Conjugation with PEG followed by folic acid

Conjugation of SA-BA acid with PEG was done using a very simple technique. For this purpose PEG having molecular weight of 6000 was used. At first, 10 mg of BA was dissolved in 20 ml of ethanol/water mixture (16:4) (MilliQ water was used). The mixture was kept in a shaking incubator at 37°C for 8 hours (200 rpm) followed by sonication for 1 hour to completely disaggregate self assembled fibers of BA (SA-BA). After this 2 mg of PEG was added to this mixture and again kept in an incubator at above mention condition. Then the mixture was centrifuged at 8000 g for 10 min to collect the pallet of PEG conjugated SA-BA (PEG-SA-BA). The pellet was washed three times using MilliQ water by centrifuge at 8000 g for 10 min to remove unbound PEG. The resultant conjugate was dried under reduced pressure in a hot air oven. For conjugation with folic acid (FA), 0.5 mg/ml folic acid was prepared in Milli Q water and 5 mg of dried PEG-SA-BA was dissolved in 10 ml of ethanol/water mixture (16:4) (MilliQ water was used). Five ml solution of FA was then added to 10 ml of PEG-SA-BA solution drop wise under stirring condition. Then the mixture was kept in a shaking incubator at 37°C for 24 hrs (200 rpm). Then the mixture was centrifuged at 8000 g

for 10 min to collect the pallet of FA conjugated PEG-SA-BA. The pellet was washed three times using MilliQ water by centrifuge at 8000 g for 10 min to remove FA. Then the conjugate was dried as above mention condition and stored at room temperature for further use.

3.5. Determination of encapsulation efficiency (EE) and loading capacity (LC)

A weighed amount (1mg) of dried FA-PEG-SA-BA was suspended in distilled water (2 ml) and then centrifuged at 10,000 g, followed by the collection of the supernatant. The absorbance of the supernatant solution was measured by UV spectrometer (UV-1800 Shimadzu) at the wavelengths of 185 nm (for PEG_{6000}), 546 nm (for FA) and the weight of the free and loaded PEG and FA in PEG-SA-BA and FA-PEG-SA-BA respectively was calculated using standard curve of PEG and FA. The EE and LC were calculated from the following formula:

$$EE(\%) = \frac{W_{tot} - W_{free}}{W_{tot}} \times 100$$

$$LC(\%) = \frac{W_{tot} - W_{free}}{W_n} \times 100$$

Where, W_{tot} is the total weight of PEG and FA in FA-PEG-SA-BA, W_{free} is the free PEG and FA released from PEG-SA-BA and FA-PEG-SA-BA respectively. Wn is the weight of ultimate conjugate after freeze-drying. All measurements were performed in triplicate and the mean value was reported.

3.6. In vitro FA release assay

In order to study the FA release behavior from FA-PEG-SA-BA, 2.5 mg of FA-PEG-SA-BA was suspended in 5 ml of PBS. The solution pH was adjusted to 5.4, and 7.4 and 9.0 using 0.1 M HCl and NaOH. Following incubation for 8, 12, 24, 48 hour and 72 hour the conjugate suspensions were withdrawn and the FA cleaved from conjugate was then quantified spectrophotometrically at 546 nm [43].

3.7. Physical characterization

3.7.1. Fourier transform infrared (FT-IR) spectroscopy: To determine the structural features of the samples, Fourier transform infrared (FT-IR) spectroscopy was carried out at 25 °C using a PerkinElmer FT-IR spectrometer (Spectrum Two FT-IR spectrometer, Version: 10.03.07.0112) with 64 scans for wave numbers ranging from 400 to 4000 cm^{-1} and resolution 4 cm^{-1}. KBr was used to prepare the pellet the samples [44].

3.7.2. Density functional theory (DFT) and Computation: All computations were performed using the Gaussian 09 (G09) software package, by using the Becke's three-parameter hybrid exchange functional and the Lee-Yang-Parr non-local correlation functional (B3LYP). All calculations done using 6-31G (d-p) basis set in gas phase. The geometric structure of the complex in the ground state (singlet) was fully optimized at the B3LYP level. The vibration frequency calculations were

performed to ensure that the optimized geometry represent local minima associated with positive Eigen values only.

3.7.3. Thin layer Chromatography (TLC): Identification of successful conjugation was also monitored by TLC. The solvent was poured into a rectangular chromatography glass chamber up to 1 inch level from the bottom. The spots of SA-BA, PEG, SA-BA-PEG, FA, and FA-PEG-SA-BA were applied on a TLC plate (Silica gel 60 F254, Merck, Darmstadt, Germany, 20 X 10 cm; layer thickness 250 µm) with the help of capillary tube. The distance between two spots was kept approximately 1.0 cm. The applied spots were dried at room temperature and eluted using 50% ethanol/ethyl acetate solvent system. The angle of the plate with the vertical was maintained approximately at 15°. The chromatogram was run until the polar solvent (Ethyl acetate) front migrated to about 10.0 cm. Then the plate was taken out and the solvent front was marked. The plate was dried at room temperature and visualized either under UV light or sprayed with the specific staining reagent. The colored spots were marked and the Rf value of each separated component was calculated. The plates were dried in air and chromatographic spots were visualized when exposed in iodine vapor and dipped in Phosphomolybdic acid (PMA) solution.

3.7.4. Thermogravimetry analysis (TGA/SDTA): The thermal analysis (TGA) of the material was carried out on a TGA/SDTA851e METTLERTOLEDO thermal analyzer. The samples were heated from room temperature to 600°C under flowing nitrogen atmosphere (flow rate: 40 cm3 min^{-1}) at a heating rate of 10°C min^{-1} in a platinum crucible [45].

3.7.5. X-ray diffraction analysis (XRD): The solid state dispersions of FA-PEG-SA-BA, was evaluated with X-ray powder diffraction. Diffraction patterns were obtained using an XPERT-PRO diffractometer (PANalytical Ltd., The Netherlands) with a radius of 240 mm. The Cu Kα radiation (λ =1.54060 Å) was Ni filtered. A system of diverging and receiving slits of 1° and 0.1 mm, respectively, was used. The pattern was collected with 40 kV of tube voltage and 30 mA of tube current and scanned over the 2θ range of 5–50° [45].

3.7.6. Scanning electron microscopy (SEM). The morphology of the self-assemblies were analyzed by high resolution scanning electron microscopy (Hitachi S-3400N). In brief sample was dissolved in ethanol: water mixture (16:4, 0.5%w/v) and then the sample was sonicated using a sonicator bath (REMI) until the sample formed a homogeneous suspension. The aliquot of the sample was deposited on a glass cube, dried in air and then by high vacuum pump. All samples were coated with a thin layer of gold before SEM examination [43].

3.7.7. ^{1}H NMR analysis: About 10 mg of SA-BA, PEG, FA, PEG-SA-BA and FA-PEG-SA-BA compounds were dissolved in $CDCl_3$ or DMSO-d_6 liquid and spectrums were run using a 300 MHz Bruker NMR instrument.[23]

3.7.8. Dynamic light scattering (DLS) and Zeta potential analysis: DLS and Zeta potential of FA-PEG-SA-BA was done by Zetasizer Nano ZS (Malvern Instruments) [43]. The FA-PEG-SA-BA was (200 µg/ml) sonicated for 10 min and dynamic particle sizes were measured by suspending two drops of aqueous suspension of FA-PEG-SA-BA in 1 ml of Millipore

water. When particle was completely dispersed in water, then particles were analyzed with a dynamic light scattering analyzer. The obtained z-average value was noted as average size of the conjugate. Zeta potential was also performed in the same instrument by universal Zeta dip cell using the same solution used for DLS study.

3.8. Cell lines culture and maintenance

The two human myeloid leukemia cell lines, KG-1A (AML), K562 (CML) RAW 264.7 (murine peritoneal macrophage) were obtained from NCCS, Pune (India). These cell lines were cultivated and maintained in IMDM, RPMI-1640 and MEM complete media respectively, each cell line, supplemented with 10% heat-inactivated fetal bovine serum (FBS), 2 mM L-glutamine, 100 U/ml penicillin, 100 μg/ml streptomycin under 5% CO2 and 95% humidified atmosphere at 37°C in CO_2 incubator. Cells were cultured and maintained in logarithmic growth phase until number of cells reaches at 1.0×10^6 cells/ml [44].

3.9.1. Selection of human subjects for collection of lymphocytes

For collection of human peripheral blood lymphocytes (PBL), six healthy subjects were chosen to collect the blood sample. The subjects enrolled in this study were asymptomatic and none of them had abnormality on physical examinations and routine laboratory tests. They were from same geographical area with same economic status, nonsmokers and non-alcoholic, and having same food habit. None of them received no medication, including vitamin-E and vitamin C for a long period of time. All subjects gave informed consent. The selection excluded not only individuals with acute infections or chronic diseases, but also excluded healthy individuals undergoing supplementation with antioxidants. The study protocol was in accordance with the declaration of Helsinki, and was approved by the ethical committee of Vidyasagar University [44].

3.9.2. Isolation of peripheral blood lymphocytes

Blood samples were collected from these six healthy human volunteers by vene-puncture in 5 ml heparin coated Vacutainers satisfying the method of Hudson and Hay [46]. Five milliliters of blood were diluted 1:1 with phosphate buffered saline (PBS) and layered onto Histopaque 1077 (Sigma) by using a Pasteur pipette and centrifuged at 400 x g (1500 rpm) for 40 min at room temperature. The upper monolayer of buffy coat i.e lymphocytes was transferred using a clean Pasteur pipette to a clean centrifuge tube and washed three times in balanced salt solution. The peripheral blood lymphocytes (PBL) were resuspended in RPMI complete media supplemented with 10% FBS and incubated for a day at 37°C in a 95% air/5% CO_2 atmosphere in CO_2 incubator. As KG-1A cells are proliferative cells, so PBL was stimulated with 1μg/ml LPS for 1 hour, followed by washing prior to most of the experiments [47].

3.10. Drug preparation

A 10 mg/ml stock of PEG-SA-BA and FA-PEG-SA-BA was prepared by dissolving 10 mg of these conjugates in ethanol-water mixture (16:4) which revealed self assembled configuration. Stock concentrations of PEG-SA-BA and FA-PEG-SA-BA were then serially diluted with RPMI media to prepare working concentrations. The amount of ethanol for each concentration, was never exceeded >0.75%.

3.11. Experimental design

Each type of cells was divided into 10 groups. Each group contained 6 petri dishes (2×10^5 cells in each). KG-1A, K562 and PBL were exposed to varying concentration (0, 1, 5, 10, 15, 20 and 25) of PEG-SA-BA, FA-PEG-SA-BA and standard drug doxorubicin for 24 hrs. After the treatment schedule the cells were collected from the petri dishes separately and centrifuged at 2,200 RPM for 10 min at 4°C to separate cells and sups [48]. The cells were washed twice with 50 mM PBS, pH 7.4. A required amount of cells were lysed using hypotonic lysis buffer (10 mM TRIS, 1 mM EDTA and Titron X-100, pH 8.0) for 45 min at 37°C and then processed for the biochemical estimation. Intact cells were used for mitochondrial membrane potential, ROS, and different microscopic observations.

3.12. In vitro cell viability assay

The dose and duration dependent cytotoxicity of PEG-SA-BA, FA-PEG-SA-BA and doxorubicin on PBL, KG-1A and K562 cell lines were quantitatively estimated by a non-radioactive, colorimetric assay system using tetrazolium salt, 3-[4,5-dimethylthiazol- 2-yl]-2,5-diphenil-tetrazolium bromide (MTT) [44]. The percentage of proliferation was calculated by using the following equation:

$$\% \text{ Proliferation} = [OD_{sample} - OD_{control}] \times 100/OD_{control}$$

The concentration required for a 50% inhibition of viability (IC_{50}) was determined graphically. Multiple linear regressions were used to compare data using Statistica version 5.0 (Statsoft, India) software package.

3.13. In vitro drug uptake Assay

To find out the internalization of PEG-SA-BA and FA-PEG-SA-BA on PBL and leukemic cell lines we performed in vitro drug uptake assay using fluorescence microscopic imaging. Briefly, Rhodamin B (Rh-B) labeled PEG-SA-BA and FA-PEG-SA-BA was prepared through the following process. Ten micrograms/ml PEG-SA-BA and FA-PEG-SA-BA were conjugated with 50 μl (2 mg/ml) of Rh-B separately. The mixture was stirred for 24 hours at 37°C using magnetic starrier (REMI, India). Then, these fluorolabeled PEG-SA-BA (PEG-SA-BA+Rh-B) and FA-PEG-SA-BA (FA-PEG-SA-BA+Rh-B) was separated by centrifugation (5000 rpm) at 4°C. The obtained sediment was washed with de-ionized water and re-dispersed. This process was repeated three times to remove the un-bounded Rh B. To determine successful tagging of Rh B on SA-BA, we examined this fluorolabeled compound under fluorescence-polarized microscopically. Finally, the obtained Rh B labeled SA-BA was dispersed in culture medium for in vitro experiment. PBL and leukemic cells (KG-1A and K562) were plated at a density of 2×10^5 cells/Petridis (35 mm) for 24 hours. Rh-B tagged FA-PEG-SA-BA at 15 μg/ml conc. respectively, were incubated for 6h at 37°C in a 95% air/5% CO_2 atmosphere in CO_2 incubator. After defined time, the cover slips were removed; the cells were washed 2 times with PBS and immediately observed in green light under the fluorescence microscope (NIKON ECLIPSE LV100POL) for

uptake assessment. Images were acquired at 50x optical zoom and analysis was done using ImageJ software v.r. 1.43 (NIH).

3.14. Hemolysis assay

For hemolysis assay of FA-PEG-SA-BA, EDTA-stabilized human blood samples were freshly obtained from healthy subjects according to the Hay protocol [46]. Five milliliters of blood sample were added to 10 ml of phosphate-buffered saline (PBS), and were centrifuged at 2,200 rpm for 10 min to obtain RBCs. The RBCs were further washed five times with 10 ml of PBS solution. The purified blood was diluted to 50 ml with PBS. Prior to PEG-SA-BA and FA-PEG-SA-BA exposure, the absorption spectrum of the positive control supernatant was checked and used only if the observance was in the range from 0.50 to 0.55 optical density units to reduce differences in samples from different donors. For the positive and negative controls set, RBC was incubated with deionized water and with PBS respectively. Then, 0.2 ml of diluted RBC suspension was added to 0.8 ml of FA-PEG-SA-BA solutions at systematically varied concentrations and mixed gently. The FA-PEG-SA-BA suspended in PBS solutions with different concentrations was prepared immediately before RBC incubation by serial dilution. All the sample tubes were kept in the static condition at room temperature for 3 h. Finally, the mixtures were centrifuged at 10,000 rpm for 3 min, and 100 µL of supernatant from all samples was transferred to a 96-well plate. The absorbance of the supernatants at 570 nm was determined by using an ELISA microplate reader (Bio-rad, India) with the absorbance at 655 nm as a reference [49]. The percent hemolysis of RBCs was calculated using the following formula:

Hemolysis (%) = $(A_{sample} - A_{negative\ control})$ / $(A_{positive\ control} - A_{negative\ control}) \times 100$,

Where A_{sample}, $A_{negitive\ control}$ and $A_{positive\ control}$ are denoted as absorbencies of the sample, and negative and positive controls, respectively. All hemolysis experiments were carried out in triplicate.

3.15. Interaction of particles with macrophages *in vitro*

RAW 264.7 cell line was used for estimation of phagocytic uptake of FA-PEG-SA-BA. The cell line was cultured in complete MEM media and allowed to adhere to the petri plate surface. RAW 264.7 cells (2×10^5) in 2 ml complete MEM media was exposed to 15 µg of FA-PEG-SA-BA-RhB and incubated for 6 hours at 37 °C in a humidified incubator. After incubation, the Petri plates were washed with warm PBS and phagocytic uptake was visualized using phase-contrast, fluorescence inverted microscope (NIKON ECLIPSE LV100POL) at ×400 magnifications [43].

3.16. Lactic dehydrogenase (LDH) releases assay

LDH release was estimated using the LDH assay kit (Reckon Diagnostics Pvt. Ltd, India) to evaluate cell membrane integrity. The values of the LDH released by the cells and FA-PEG-SA-BA treated cells found in the culture supernatants were determined by spectrophotomatically. PBL, KG-1A and K562 cells were seeded in a 96-well plate at a density of $(2 \times 10^4$ cells/well) and incubated with or without FA-PEG-SA-BA (15 µg/ ml) freshly dispersed in culture medium for 24 hours. After

that, 50 µl of culture supernatant were used for LDH measurement according to manufacturer's instruction.

3.17. Intracellular ROS measurement and effect of ROS quencher pre-treatment

ROS measurement was performed using H_2DCFDA according to our previously reported method [44]. In brief, Normal PBL, KG-1A and K562 cell lines $(2X\ 10^5$ cells per milliliter) were treated with FA-PEG-SA-BA at 15 µg/ml for 24 hours. As a positive control, those cells were incubated with H_2O_2 (100 µM) for 30 min prior to the analysis [50]. After treatment schedule cells were washed with culture media followed by incubation with 1 µg/ml H_2DCFDA for 30 min at 37ºC. Then the cells were washed three times with fresh culture media. DCF fluorescence was determined at 485 nm excitation and 520 nm emission using a Hitachi F-7000 Fluorescence Spectrophotometer and was also observed by fluorescence microscopy (NIKON ECLIPSE LV100POL). All measurements were done in triplicate. To determine the role of ROS in FA-PEG-SA-BA induced cell death, KG-1A and K562 cells were seeded in a 96-well plate at 0.2 mL per well at a concentration of 2 X 10^5 cells per milliliter. A stock solution of N-acetyl- L-cysteine (NAC; Sigma- Aldrich) was made with sterile water and added to cells at 5 and 10 mM for 1 h. NAC is a potent scavenger for ROS production. After NAC pretreatment, cells were cultured with FA-PEG-SA-BA (15 µg/ml) for 24 h. Viability was determined by the MTT method [44].

3.18. Measurement of mitochondrial membrane potential (ΔΨm)

The alteration of mitochondrial membrane potential by Spectro-fluorometric method was done according to our previous reported method [51]. In brief, PBL, KG-1A and K562 cell lines $(2X\ 10^5$ cells per milliliter) were treated with DOX and FA-PEG-SA-BA at 15 µg/ml dose for 12 hours. It was evident from the previous study that DOX can decrease mitochondrial membrane potential significantly [52]. After treatment schedule cells were washed with culture media followed by incubation with 1.5 µM Rhodamin 123 for 10 min at 37ºC in a humidified incubator. Then the cells were washed three times with culture media. The cellular fluorescence intensity of Rh 123 was monitored for 2 min using Hitachi F-7000 Fluorescence Spectrophotometer. A required amount of cells was also used for microscopic observations (NIKON ECLIPSE LV100POL). The cellular mitochondrial membrane potential was expressed as fold change with compare to control cells at an excitation wavelength of 493 nm and an emission wavelength of 522 nm. Both excitation and emission slit width were set to 5.0.

3.19. Apoptotic morphological changes by AO/ Et-Br and DAPI staining

Two DNA-binding dyes AO and Et-Br were used for the morphological apoptotic and necrotic cells [53]. After treatment with a 15µg / ml dose of FA-PEG-SA-BA for 24 h, the PBL and KG-1A and K562 cells were isolated, washed with cold PBS and then stained with a mixture of AO (100µg/ml) and Et-Br (100µg/ml) at room temperature for 5 min. After proper washing with PBS, the stained cells were observed by a fluorescence microscope at 40× magnifications.

For DAPI staining, all the test cells were seeded into six well plates. A number of 2×10^5 cells/ml were treated with or without FA-PEG-SA-BA (0, and 15) for 24 hours and were then isolated for DAPI staining according to the modified method of Mollick et al. [53]. After treatment, the cells were fixed with 2.5% glutaraldehyde for 15 min, permeabilized with 0.1% Triton X-100 and stained with 1 µg/ml DAPI for 5 min at 37°C. The cells were then washed with PBS and examined by fluorescence microscopy (NIKON ECLIPSE LV100POL).

3.20. Assessment of apoptotic cell population by Annexin V/PI double-staining assay

Cells (1×10^6) were seeded in Petri discs and incubated for 24 hours at 37°C. Then FA-PEG-SA-BA (0, and 15) was directly added to the dishes and incubated for an additional 24h, respectively. After FA-PEG-SA-BA, PBL, KG-1A and K562 cells were collected, washed with PBS and resuspended in PBS. Apoptotic cell death was identified by double staining with recombinant FITC-conjugated Annexin V and PI, using the Annexin V-FITC Apoptosis Detection kit (E-bioscience, India) according to the manufacturer's instructions. Flow cytometric analysis was performed immediately after dual staining. Data acquisition and analysis were performed in a Becton-Dickinson FACS verse flow cytometer using CellQuest software.

3.21. Estimation of TNF-α level and Co-culture with pentoxifylline

The level of TNF- α, in serum free culture supernatants were measured using an enzyme-linked immunosorbent assay (ELISA) kit with pre-coated plates (Human TNF alpha ELISA Ready-SET-Go, E-bioscience, India) according to manufacturer's instruction. In brief, PBL and KG-1A and K562 cells were treated with FA-PEG-SA-BA (15 µg/ml) and 1 µg/ml LPS for 24 hrs. It was found from the previous study that, LPS is one of potential stimulator for cytokines releases from various types of cells [54]. After treatment culture supernatants were separated by centrifugation (2200 rpm for 10 min). Hundred micro liter of each supernatant were taken as sample for cytokines release level. O.D was recorded using an ELISA micro plate reader, Bio Rad, India. The sensitivity limits was 4.0 pg/ ml for TNF- α, cytokine. Cytokine concentration was expressed as pg/ml/10^6 cells to correct for the number of total PBL, KG-1A and K562 cells. To understand potential contribution of TNF-α in FA-PEG-SA-BA induced cell death, PBL, KG-1 and K562 cells were co-cultured with 1mM and 2 mM Pentoxifylline (a potent TNF-a inhibitor) with 15 µg/ml dose of SA-BA for 24 hrs. The doses of pentoxifylline were selected from the previous study of Dash et al [44]. After the treatment schedule cells were washed two times with culture medium and cell viability was estimated by MTT assay [44].

3.22. Immunofluorescent staining

Both the KG-1A and K562 cells were treated with 15µg/ml of FA-PEG-SA-BA for 24 h. At the end of treatment(s), the cells were washed with PBS, pH 7.2, and were fixed in 4% paraformaldehyde solution for 15 min at 4°C. Next, the cells were washed three times with the blocking buffer (5% bovine serum albumin in PBS), followed by permeabilization with 0.5% Triton X-100 in PBS for 20 min at 25°C. After three washes with the blocking buffer, the cells were incubated for 1 h at 250 C with human antibodies specific for caspase-8, 3. The antibodies were used at dilutions of 1:100, in blocking buffer. The cells were then rinsed three times with the blocking buffer and probed in the dark with rhodamin-conjugated compatible secondary antibodies for 1 h at 250C. Following three washes with the blocking buffer, the cover slips were mounted on glass slides using a Fluoromount G (Electron Microscopy Sciences, Fort Washington, Pa., USA). The slides were viewed using a fluorescence microscope (NIKON ECLIPSE LV100POL) equipped with the suitable wavelength filters [55].

3.23. Protein estimation

Protein was determined according to Lowry et al., 1951 using bovine serum albumin as Standard [56].

3.24. Statistical analysis

All the parameters were repeated at least three times. The data were expressed as mean ± SEM, n = 06. Comparisons between the means of control and treated group were made by one-way ANOVA test (using a statistical package, Origin 6.1, Northampton, MA 01060 USA) with multiple comparison t tests, $p < 0.05$ as a limit of significance.

4. Conclusion

In this study, a simple and economically viable method has been adopted to prepare FA-PEG-SA-BA. The physiochemical characterization clearly demonstrates that the synthesized material conserved its self assembly property ever after conjugation with FA and PEG. The fibrillar networks of FA-PEG-SA-BA preferentially targeted higher FR expressing K562 cells with comparatively lower internalization on lower FR expressing KG-1A cells. Thus, FA-PEG-SA-BA showed higher effectiveness towards K562 cells and the significant effects on KG-1A was due to the self assembled configuration of the conjugate. On the other hand FA-PEG-SA-BA did not show any toxic effects on PBL and RBCs due to its very minimum internalization. Selective cytotoxicity of FA-PEG-SA-BA on leukemic cells occurred by the alteration of cellular redox balance, disruption of mitochondrial outer membrane potential and thereby induction of apoptosis phenomenon. Induction of apoptosis in both leukemic cell lines through activation of upstream caspases (Caspase 3 and 8) was observed. The present study revealed that the involvement of ROS followed by TNF-α is the major contributors of FA-PEG-SA-BA induced leukemic cell death through apoptosis mechanism. Hence, for the first time this study elicited the probable targeted delivery approach of SA-BA towards FR over expressing cells, can be used as a lead molecule for generation of drugs in leukemia treatment and management.

Acknowledgements

Notes and references

1. V. Zuco, R. Supino, S. C.Righetti, L. Cleris, E. Marchesi, C.Gambacorti-Passerini, and F. Formelli, *Cancer. Lett.,* 2002, **175**(1), 17-25.

2. S. Fulda, *Int. J. Mol. Sci.,* 2008, **9**(6), 1096–1107.

3. M. GhaffariMoghaddam, F. Bin H. Ahmad and A. Samzadeh-Kermani, *Pharmacoland Pharmacy*, 2012, **3**(2), 119-123.

4. D. V. RaghuvarGopal, A. A. Narkar, Y. Badrinath, K. P. Mishra and D. S. Joshi, *Toxicol. Lett.,* 2005,**155**(3), 343-351.

5. E. D. Clercq, *Curr. Med. Chem.* 2001, **8**, 1543–1572.

6. Y. Tan, R. Yu and J. M. Pezzuto, *Clin. Cancer. Res.,* 2003,**9**, 2866–2875

7. D. Thurnher, D. Turhan, M. Pelzmann, et al, 2003, *Head and Neck* **25** (9), 732–740.

8. S. Fulda and G. Kroemer, *Drug. Discov. Today.,* 2009, **14**(17-18), 885-890.

9. X. Zhao, H. Li and R. J. Lee, *Expert. Opin. Drug. Deliv.,* 2008,**5**(3), 309-319.

10. H. Ehrhardt, S. Fulda, M. Führer, K. M. Debatin and I. Jeremias, *Leukemia,* 2004, **18**(8), 1406-1412.

11. H. S. Yoo and T. G. Park, *J. Control. Release.,* 2004, **100**(2), 247-256.

12. A. R. Hilgenbrink and P. S.Low, *J Pharm Sci.* 2005, **94**(10), 2135-2146.

13. O. Issarachot, J. Suksiriworapong, M. Takano, R. Yumoto and V. B. Junyaprasert, *J. Nanopart. Res.,* 2014, **16**, 2276.

14. H. Elnakat and M. Ratnam, *Adv. Drug. Deliv. Rev.,* 2004, **56**, 1067-1084.

15. D. J. O'Shannessy, E. B. Somers, E. Albone, X. Cheng, Y. C. Park, B. E. Tomkowicz, Y. Hamuro, T. O. Kohl, T. M. Forsyth, R. Smale, Y. S.Fu and N. C.Nicolaides, *Oncotarget*, 2011, **2**(12), 1227-1243.

16. R. I. E Gogary, N. Rubio, J. T. Wang, W. T. A Jamal, M. Bourgognon, H. Kafa, M. Naeem, R. Klippstein, V. Abbate, F. Leroux, S. Bals, G. Van Tendeloo, A. O. Kamel, G. A. Awad, N. D.Mortada and K. T.A Jamal, *ACS Nano*, 2014, **8**(2), 1384-134401.

17. Q.Wu, J. He, J. Fang and M. Hong., *J. Huazhong. Univ. Sci. Technolog. Med. Sci.,* 2010, **30**(4), 453-457.

18. L. S. Yazan, F. H. Ahmad, O. C. Li, R. A. Rahim, H. A. HamidandL. P.Sze. *Malaysian Journal of Pharmaceutical Sciences*, 2009, **7**(1), 23–37.

19. S. K. Sahu, S. Maiti, T. K. Maiti, S. K. Ghosh and P. Pramanik, *Macromol. Biosci.,* 2011,**11**(2), 285-295.

20. S. Yamamura and Y. Momose, *Int. J. Pharm.,* 2001, **212**, 203–212.

21. C. Soica, C. Danciu, G. Savoiu-Balint, F. Borcan, R. AmbrusIstvanZupko, F. Bojin, D.Coricovac, S. Ciurlea, S. Avram, C. Adriana Dehelean, T.Olariu and P Matusz. *Int. J. Mol. Sci.* 2014, **15**, 8235-8255

22.G. Motkar, M. Lonare, O. Patil, and S. Mohanty, *AIChE. Journal*, 2013, **59**(4), 1360-1368.

23. B. G. Bag and S. S. Dash, *Nanoscale*, 2011, **3**(11):4564-4566

24. S. Chattopadhyay, S. K. Dash, T. Ghosh, S. Das, S. Tripathy, D. Mandal, D. Das, P. Pramanik and S. Roy, *J. Biol. Inorg. Chem.,* 2013, **18**(8), 957-973.

25. N. H. Faujan, N. B. Alitheen, S. K. Yeap, A. M. Ali., A. H. Muhajir and F. B. H. Ahmad, *African J. Biotechnol.,* 2010, **9**(38), 6387-6396.

26. W. Rzeski, A. Stepulak, M. Szymanski, M. Sifringer, J. Kaczor, K. Wejksza et al, *NaunynSchmiedebergs. Arch. Pharmacol.,* 2006, **374**, 11-20.

27. S. Mohapatra, S. K. Mallick, T. K. Maiti, S. K. Ghosh and P. Pramanik, *Nanotechnology,* 2007, **18**, 385102–385111.

28. M. Gao, P. M. Lau and S. K. Kong. *Arch. Toxicol.,* 2014, **88**(3), 755-768.

29. G. Fontana, M. Licciardi, S. Mansueto, D. Schillaci andG. Giammona, *Biomaterials*, 2001, **22**(21), 2857-2865.

30. B. A. Kamen and A. K. Smith, *Adv. Drug. Deliv. Rev.,* 2004, **56**, 1085–1097.

31. M. Das, D. Mishra, T. K. Maiti, A. Basak and P. Pramanik, *Nanotechnology,* 2008, **19**, 415101.

32. S. Gurunathan, J. Raman, S. N. A. Malek, P. AJohn andS. Vikineswary.*Inter. J. Nanomed.,* 2013, **8**, 4399–4413.

33. M. M. Wang, N. Z. Zhang, F. X. Chen, J. Q. Liu, Z. H. Zhou and J. Zhang. *Chinese J.Microbiol and Immunol,* 2012, **32** (1).

34. V. Viji ,A. Helen andV. R. Luxmi. *British. J. of Pharmacol.,* 2011,**162**,1291–1303.

35. A. Ganguly, B. Das, A. Roy,N.Sen, S. B. Dasgupta, S. Mukhopadhayay and H. K. Majumder, *Cancer. Res.,* 2007, **67**(24), 11848.

37. J. A. Collins, C. A. Schandl, K. K. Young, J. Vesely and M. C. Willingham, *J. Histochem. Cytochem.,* 1997, **45**, 923-934.

38. S. Yang, N. Liang, H Li, W. Xue, D. Hu, L. Jin, Q. Zhao and S. Yang, *Chemistry Central J.,* 2012, 6, 141.

39. M. J. Morgan and Z. G. Liu. *Mol. Cells.,* 2010, **30**, 1-12.

40. H. Kamata, S. Honda, S. Maeda, L. Chang, H. Hirata and M. Karin, *Cell.,* 2005, **120**(5), 649-661.

41. J. J Kim, S. B Lee, J. K. Park and Y. D. Yoo, *Cell. Death. Differ.,* 2010, **17**, 1420-1434.

42. L. Wang, F. Du and X. Wang, *Cell.,* 2008, **133**(4), 693-703.

43. S. Chattopadhyay, S. K. Dash, T. Ghosh, D. Das, P. Pramanik and S. Roy, *Cancer. Nano.,* 2013, **4,** 103–116.

44. S. K. Dash, T. Ghosh, S. Roy, S. Chattopadhyaya and D. Das, *J. Appl. Toxicol,.* 2014, Doi: 10.1002/jat.2976.

45. T. Ghosh, S. K. Dash, P. Chakraborty, A. Guha, K. Kawaguchi, S. Roy, T. Chattopadhya, and D. Das, *RSC. Adv.,* 2014, **4**(29), 15022-15029.

46. L. Hudson and F. C. Hay, in *Practical Immunology*, Blackwell Publishing, Oxford, UK, 3rd edn., 1989.

47. T. Mattern, H. D. Flad, L. Brade, E. T. Rietschel and A. J. Ulmer, *J. Immunol.,* 1998, **160**(7), 3412-3418.

48. S. Chattopadhyay, S.P. Chakraborty, D. Laha, R. Baral, P. Pramanik, S. Roy, *Cancer Nano.,* 2012, **3**(1-6), 13-23.

49. S Chattopadhyay, S. K. Dash, S. KarMahapatra, S. Tripathy, T. Ghosh, B. Das, D. Das, P. Pramanik and S. Roy. *J. Biol. Inorg. chem.,* 2014, **19**(3), 399-414.

50. J. S. Armstrong, K. K. Steinauer, B. Hornung, J. M. Irish, P. Lecane, G. W. Birrell, D. M. Peehl and S. J. Knox, *Cell. Death. Differ.,* 2002, **9**(3), 252-263.

51. S. K. Dash, S. Chattopadhyay, T. Ghosh, S. Tripathy, S. Das, D. Das and S. Roy, ISRN. Oncol., 2013, Article ID 709269.

52. X. Lv, X. Yu, Y. Wang, F. Wang, H. Li, Y. Wang, D. Lu, R. Qi and H. Wang, *PLoS. One.,* 2012, **7**(10), e47351.

53. R. M. M. Mollick, B. Bhowmick, D. Mondal, D. Maity, D. Rana, S. K. Dash, S. Chattopadhyay, S. Roy, J. Sarkar, K. Acharya, M. Chakraborty and D. Chattopadhyay, *RSC. Adv.,* 2014, DOI: 10.1039/c4ra07285e.

54. R. A. Frost, G. J. Nystrom and C. H. Lang. *Am. J. Physiol. RegulIntegr. Comp. Physiol.,* 2002, **283**(3), R698-709.

55. S. G. Joshi and S. K. Sahni, *Histoche. and cell boil.,* 2003, **119**(6), 463-68.

56. O. H. Lowry, N. J. Rosebrough, A. L. Farr and R. J. Randall, *J. Biol. Chem.,* 1951, **193**(1), 265-75.

57. T. Chattopadhyay, M. Mukherjee, A. Mondal, P. Maiti, A. Banerjee, K. S. Banu, S. Bhattacharya, B. Roy, D. J. Chattopadhyay, T. K. Mondal, M. Nethaji, E. Zangrando, D. Das. Inorg Che., 2010, 49(7), 3121-9. doi: 10.1021/ic901546t.